Evaluation of Composite TiO_2-$FeTiO_3$ Coatings Prepared by Plasma Spraying Technique†

YE Fuxing*, OHMORI Akira**

Abstract

The composition and photocatalytic activity of plasma sprayed $FeTiO_3$, TiO_2-30%$FeTiO_3$ and TiO_2-50%$FeTiO_3$ coatings were investigated. The influence of $FeTiO_3$ compound on the charge carrier separation and recombination in TiO_2-$FeTiO_3$ coatings was clarified. The TiO_2-30%$FeTiO_3$ coating sprayed under an arc current of 400A, and contained anatase TiO_2, rutile TiO_2 and $FeTiO_3$, had good photocatalytic activity because the coating did not contain the unfavorable Fe_2TiO_5 phase. However, the relative deposition speed of TiO_2-30%$FeTiO_3$ powder under an arc current of 400A approximated to 4 μm/pass, which was very low. Although pure $FeTiO_3$ compound nearly did not show photocatalytic performance, the existence of $FeTiO_3$ could improve the photocatalytic activity of anatase TiO_2 if $FeTiO_3$ contacts coherently with TiO_2, and this was explained using a two-steps electron transfer model.

KEY WORDS: (Plasma spraying), (Photocatalytic activity), (TiO_2), ($FeTiO_3$), (Fe_2TiO_5)

1. Introduction

Titanium-substituted iron oxides are widespread in nature and represent an important mineral resource for the commercial extraction of both iron and titanium[1]. The $FeTiO_3$ structure, which is of rhombohedral crystal structure, is derived from α-Fe_2O_3 by replacing every other layer of the Fe atoms in (0001) planes by a layer of Ti atoms[2, 3]. Ilmenite is an incongruently melting material with a melting point of approximate 1683K[4]. Although the high temperature electrical conductivity and magnetic properties of ilmenite $FeTiO_3$ have been investigated in detail[2-6], very little work has been done on its performance as a chemical catalyst and photocatalyst[7]. Characterization of the photocatalytic performance of TiO_2-$FeTiO_3$ composites has not been reported until now.

To elucidate the influence of $FeTiO_3$ on the photocatalytic activity of plasma sprayed TiO_2-Fe_3O_4 coatings, $FeTiO_3$ and TiO_2-$FeTiO_3$ powders were used. The phase composition, microstructure and photocatalytic activity of plasma sprayed $FeTiO_3$, TiO_2-30%$FeTiO_3$ and TiO_2-50%$FeTiO_3$ coatings were examined in detail. The photocatalytic activity of TiO_2, TiO_2-30%$FeTiO_3$ and $FeTiO_3$ powders was also evaluated.

2. Materials and experimental procedures

2.1 Feedstock powders and substrate

$FeTiO_3$ particles with average size of 1.4μm were agglomerated to $FeTiO_3$ feedstock powder with an average size of 32.5μm. To manufacture TiO_2-30%$FeTiO_3$ and TiO_2-50%$FeTiO_3$ feedstock powders, TiO_2 particles with an average size of 0.2μm were mechanically and uniformly mixed with 1.4μm $FeTiO_3$ particles and corresponding weight ratios. The average sizes of TiO_2-30%$FeTiO_3$ and TiO_2-50%$FeTiO_3$ powders were 30.4μm and 28.9μm, respectively. The X-ray diffraction patterns of the TiO_2, $FeTiO_3$, TiO_2-30%$FeTiO_3$ and TiO_2-50%$FeTiO_3$ feedstock powders are shown in **Fig.1**. The morphology of TiO_2-30%$FeTiO_3$ powder is given in **Fig.2**, and was very similar to the $FeTiO_3$ and TiO_2-50%$FeTiO_3$ powders. The substrate was stainless steel (JIS SUS304).

2.2 Plasma spraying equipment

The thermal spraying equipment was a plasma spraying system (Plasmadyne-Mach1 manufactured by Plasmadyne Company). Argon was applied as primary gas, and helium was applied as secondary gas. The thermal spraying parameters are given in **Table 1**.

2.3 Characterization of powders and sprayed coatings

An electron probe surface roughness analyzer (ERA-8800FE, Elionix Co. Ltd., Japan) and energy dispersive spectroscopy (EDS) were used to examine the structural characteristics of the feedstock powders and the sprayed coatings. The phase composition of the feedstock

† Received on July 8, 2004
* Designated Researcher
** Professor

Transactions of JWRI is published by Joining and Welding Research Institute of Osaka University, Ibaraki, Osaka 567-0047, Japan

powders and the sprayed coatings was investigated by x-ray diffraction using Cu-Kα radiation (λ=1.5406Å) and a graphite crystal monochromator (M03XHF, MAC Science Co. Ltd.). To evaluate powder deposition efficiency, the relative deposition speed of powder was calculated using Equation (1).

$$RDSP = \frac{T_{Thickness} V_{Traverse} W_{Step}}{n V_{Rotation}} \quad (1)$$

where *RDSP* is Relative Deposition Speed of Powder, $V_{Rotation}$ relative rotation speed of powder feeder, $V_{Traverse}$ relative traverse speed of plasma gun, W_{Step} relative step width of up-down moving equipment, $T_{Thickness}$ thickness of sprayed coating, *n* spray pass of the coating.

The photocatalytic activity of sprayed coatings was evaluated using an acetaldehyde degradation set-up, and the τ value was calculated using Equation (2).

$$\ln(\frac{C}{C_0}) = -t/\tau \quad (2)$$

where C is the reactant concentration, C_0 the initial concentration of reactant, t reaction time and τ photo-catalytic activity constant.

3. Results and discussion

3.1 Typical microstructures of $FeTiO_3$ and TiO_2-$FeTiO_3$ coatings

Figure 3 shows the cross sections of TiO_2- 30%$FeTiO_3$ coatings sprayed under the arc current of 400A, 600A and 800A. It indicates that the coating became denser with increasing arc current. As clearly shown in **Fig.4**, many primary particles existed in the coating sprayed under the arc current of 400A for the low energy transfer from plasma jet. The relative deposition speed of TiO_2-30%$FeTiO_3$ powder, which was approximate to 4μm/pass, had no significant variation compared to that of the TiO_2 powder as shown in **Fig.5**. With an increase of arc current to 600A or 800A, the relative deposition speed of the TiO_2-30%$FeTiO_3$ powder (RDSP) clearly increased.

Figure 6 shows the cross sections and surface morphologies of $FeTiO_3$ and TiO_2-50%$FeTiO_3$ coatings sprayed under an arc current of 400A. It indicates that the $FeTiO_3$ powder is more melted than the TiO_2-50%$FeTiO_3$ powder, which also can be inferred from **Fig.5**.

3.2 Composition of $FeTiO_3$ and TiO_2-$FeTiO_3$ coatings

The x-ray diffraction pattern of plasma sprayed $FeTiO_3$ coating under an arc current of 400A is illustrated in **Fig.7(a)**. The $FeTiO_3$ coating consisted of rutile TiO_2, $FeTiO_3$, Fe_2TiO_5, $Fe_2Ti_3O_9$ and γ-Fe_2O_3 (maghemite). Y. Chen et al.[9, 10] reported that the thermal oxidation process of $FeTiO_3$ by high energy ball milling in air consists of reactions (3)~(5). The $Fe_2Ti_3O_9$ and γ-Fe_2O_3 are thermally

Table1 Plasma spraying parameters.

Argon gas pressure (MPa) /flow (slpm)	0.42/58
Helium gas pressure (MPa) /flow (slpm)	0.21/9
Arc current (A)	400,600,800
Arc voltage (V)	28~30
Spraying distance (mm)	70

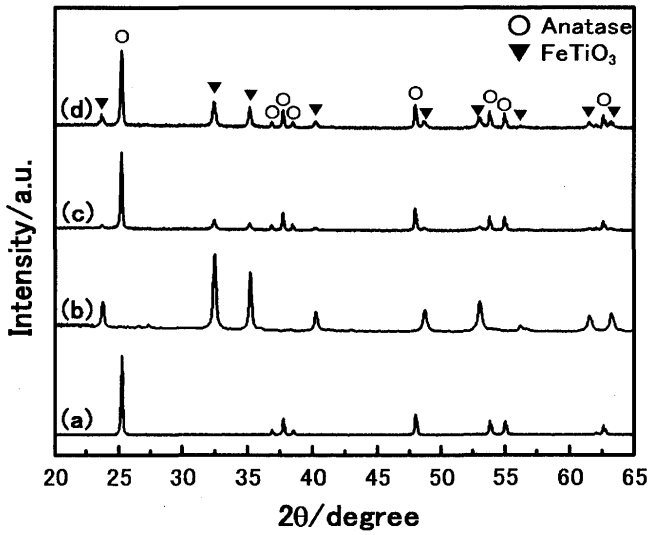

Fig.1 X-ray diffraction patterns of the TiO_2 (a), $FeTiO_3$ (b), TiO_2-30%$FeTiO_3$ (c) and TiO_2-50%$FeTiO_3$ (d) feedstock powders.

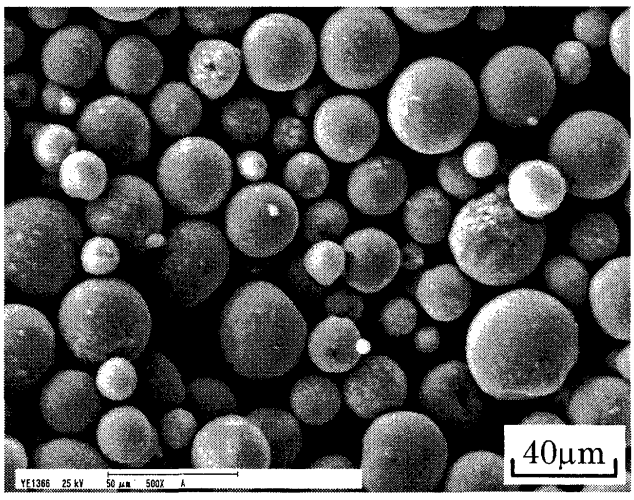

Fig.2 The morphology of TiO_2-30%$FeTiO_3$ powder.

metastable products, which are normally difficult or impossible to produce by conventional thermal equilibrium processes. These metastable phases were also observed in plasma sprayed $FeTiO_3$ coatings.

$$4FeTiO_3 + O_2 \rightarrow Fe_2Ti_3O_9 + TiO_2 + Fe_2O_3 \quad (3)$$

$$Fe_2O_3 + TiO_2 \rightarrow Fe_2TiO_5 \quad (4)$$

$$Fe_2Ti_3O_9 \rightarrow Fe_2TiO_5 + 2TiO_2 \quad (5)$$

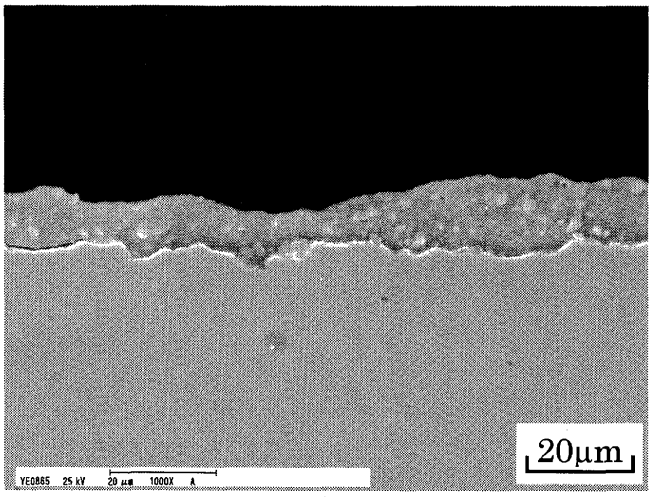

(a)

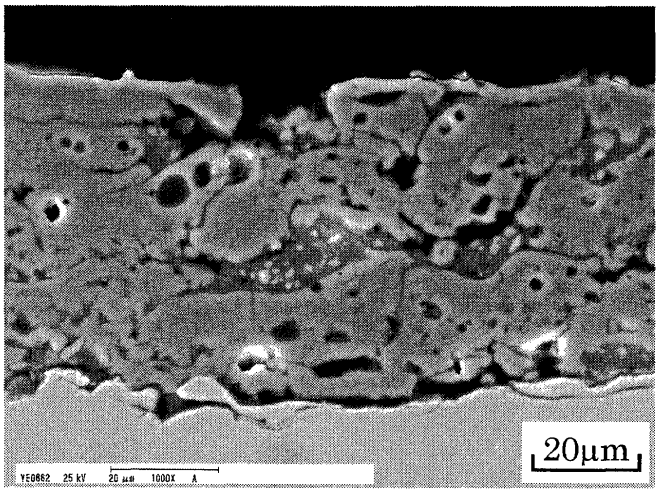

(b)

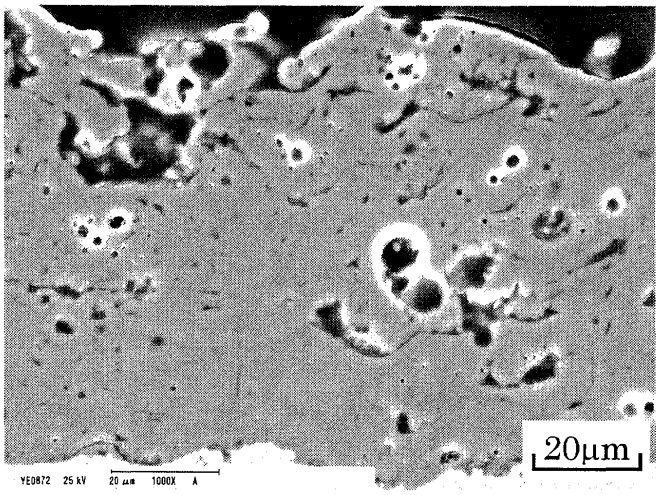

(c)

Fig.3 Cross sections of TiO_2-30%$FeTiO_3$ coatings sprayed under the arc current of 400A(a), 600A(b) and 800A(c).

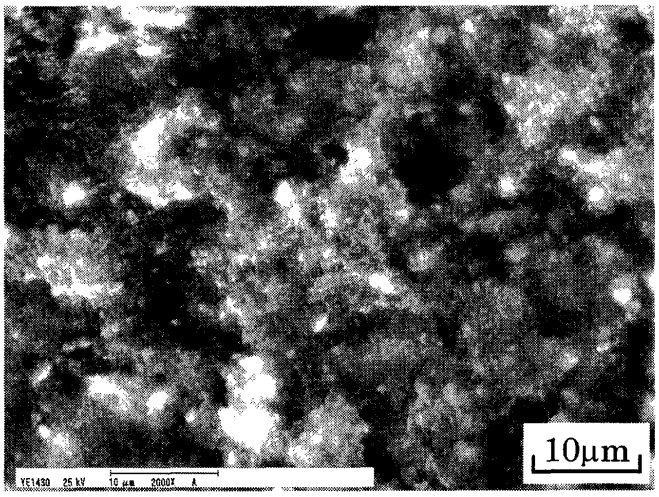

(a)

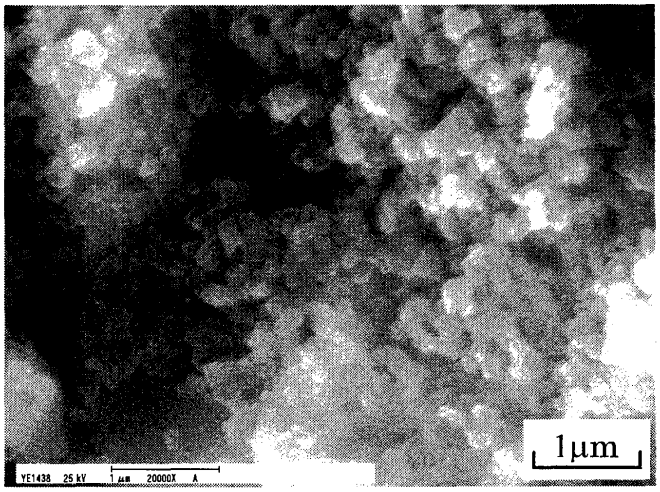

(b)

Fig.4 Surface morphologies of TiO_2-30%$FeTiO_3$ coating sprayed under the arc current of 400A ((a) low magnification, (b) high magnification.).

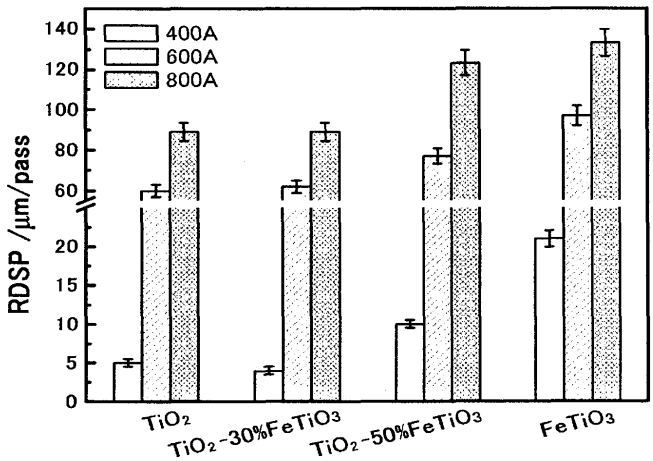

Fig.5 Relative deposition speed of TiO_2, TiO_2-30%$FeTiO_3$, TiO_2-50%$FeTiO_3$ and $FeTiO_3$ powder (RDSP) under the arc current of 400A, 600A and 800A.

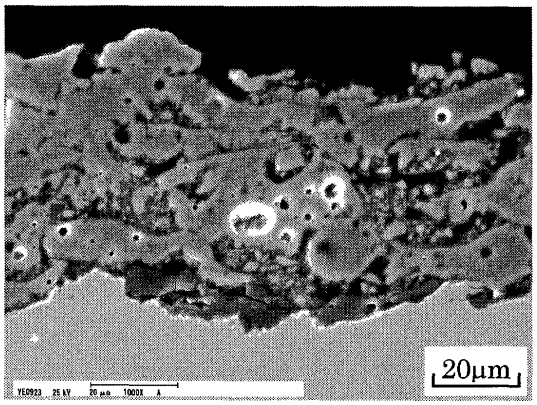

(a)

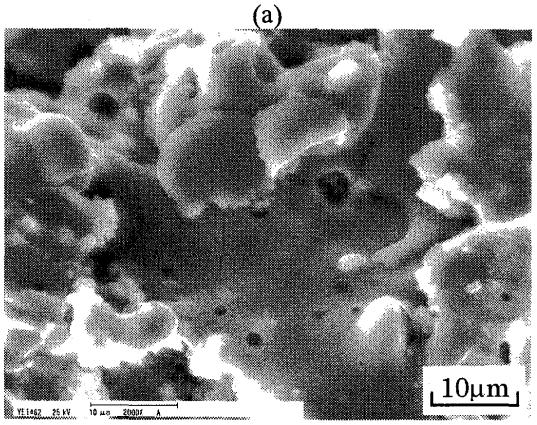

(b)

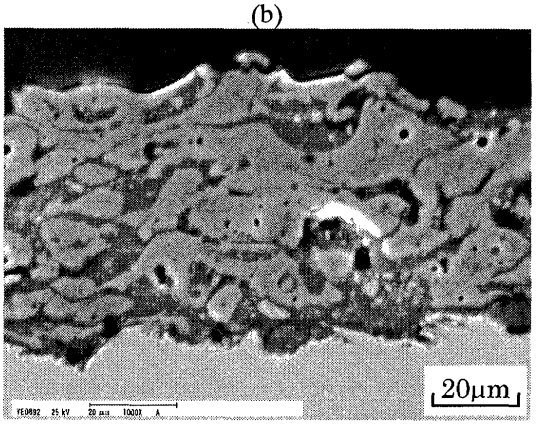

(c)

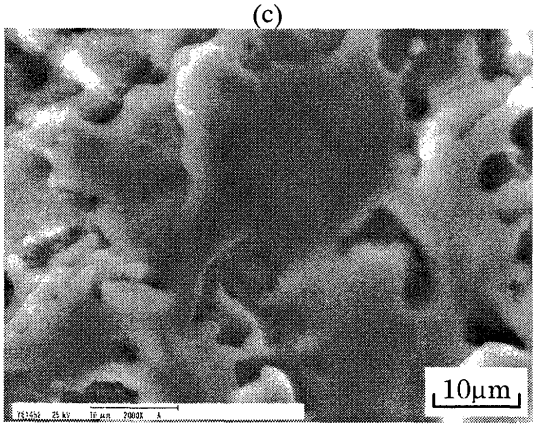

(d)

Fig.6 Cross sections and surface morphologies of $FeTiO_3$ (a, b) and TiO_2-50%$FeTiO_3$ (c, d) coatings under the arc current of 400A.

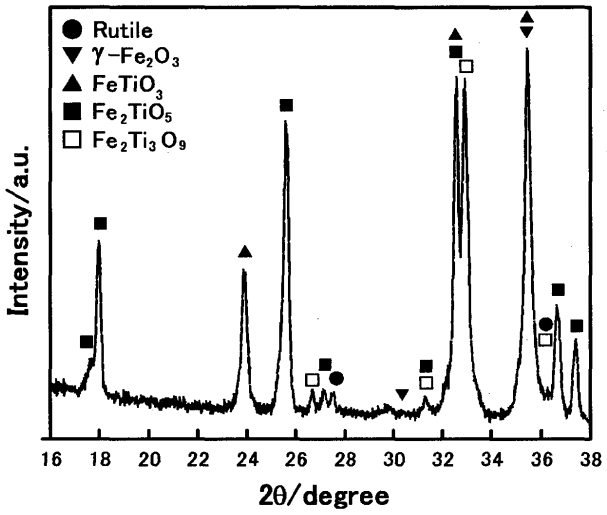

(a)

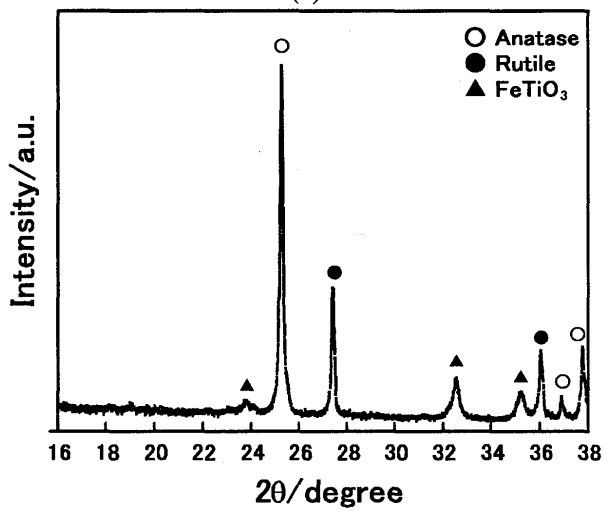

(b)

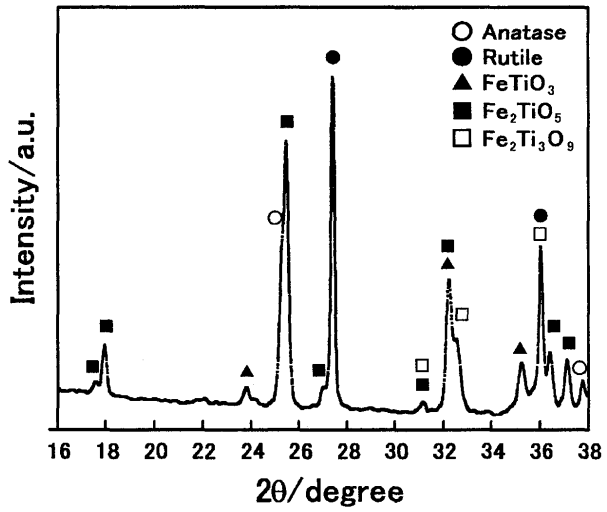

(c)

Fig.7 X-ray diffraction patterns of $FeTiO_3$ (a), TiO_2-30%$FeTiO_3$ (b) and TiO_2-50%$FeTiO_3$ (c) coatings plasma sprayed under an arc current of 400A and spraying distance of 70mm.

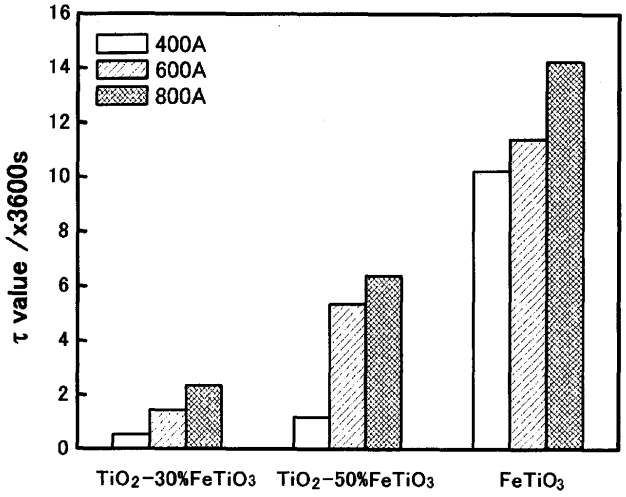

Fig.8 τ values of plasma sprayed TiO_2-30%$FeTiO_3$, TiO_2-50%$FeTiO_3$ and $FeTiO_3$ coatings under the arc currents of 400A, 600A and 800A.

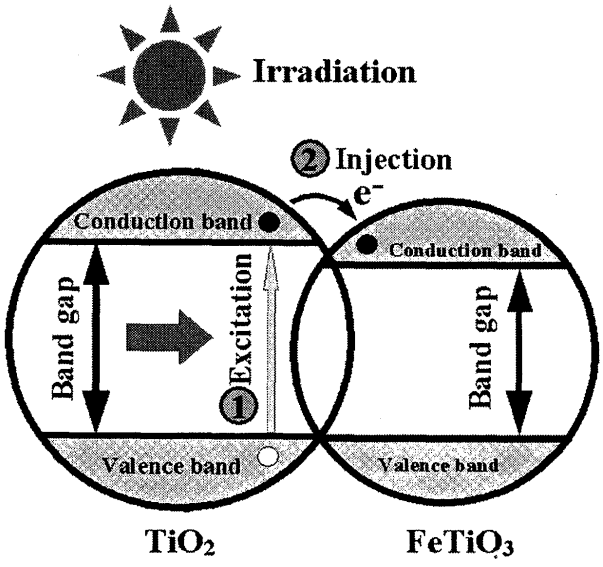

Fig.9 A proposed two-steps electron transfer model for the good photocatalytic activity of TiO_2-30%$FeTiO_3$ coating.

The TiO_2-30%$FeTiO_3$ coating under the arc current of 400A consisted of anatase TiO_2, rutile TiO_2 and $FeTiO_3$ as illustrated in **Fig.7(b)**. Under the arc current of 400A, large part of anatase TiO_2 and $FeTiO_3$ still existed, and Fe_2TiO_5 and $Fe_2Ti_3O_9$ phases were undetectable. With an increase of arc current to 600A or 800A, Fe_2TiO_5, $Fe_2Ti_3O_9$ and Fe_2O_3 phases appeared in the sprayed coatings.

With the increase of the weight content of $FeTiO_3$ to 50% in the TiO_2-$FeTiO_3$ feedstock powder, $Fe_2Ti_3O_9$ and Fe_2TiO_5 phases appeared in spite of the low arc current of 400A as illustrated in **Fig.7(c)**.

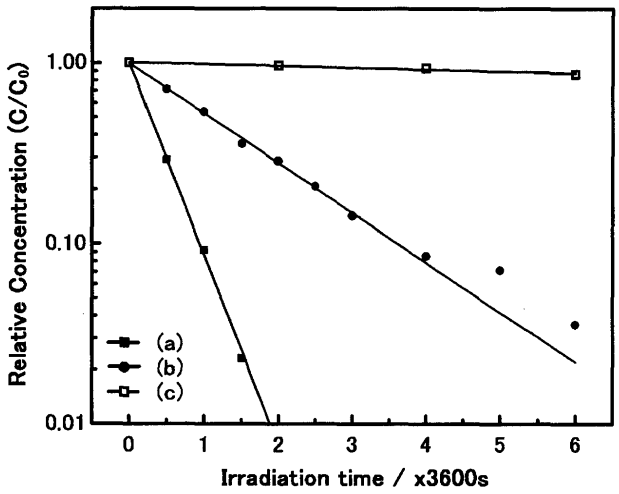

Fig.10 Decomposition characteristics of the acetaldehyde by agglomerated TiO_2 (a), TiO_2-30%$FeTiO_3$ (b), and $FeTiO_3$ (c) feedstock powders.

3.3 Photocatalytic activity of $FeTiO_3$ and TiO_2-$FeTiO_3$ coatings

The photocatalytic activity of prepared coatings was evaluated by a decomposition experiment using acetaldehyde, and the τ values of the coatings are shown in **Fig.8**. The results reveal that the $FeTiO_3$ coatings had almost no photocatalytic activity. The photocatalytic activity of the TiO_2-30%$FeTiO_3$ coating (τ=1872s) sprayed under an arc current of 400A was better than that of the TiO_2 coating (τ=2484s)[11] sprayed under the same conditions.

Because the TiO_2-30%$FeTiO_3$ coating sprayed under the arc current of 400A consisted of TiO_2 and $FeTiO_3$ only, and did not contain the unfavorable phase of Fe_2TiO_5 as discussed in **Section 3.2** and a large part of the PVA combusted at the high temperature of the plasma jet according to the EDAX analysis results, the photocatalytic activity was better than that of the other sprayed coatings.

Furthermore, the band gap of bulk $FeTiO_3$, which is 2.85eV [12], is lower than that of TiO_2. A possible explanation shows in **Fig.9**. When the semiconductor is irradiated, the electron possibly transfers (moves) to the conduction band in two steps. First step: the electron is initiated from the valence band to the conduction band of TiO_2, and in second step the electron in the conduction band of TiO_2 transfers to the conduction band of $FeTiO_3$. For this two-steps transfer mechanism, the lifetime of the excited hole and electron pair was prolonged. Perhaps the improved efficiency of the photon is another reason for the higher photocatalytic activity of the TiO_2-30%$FeTiO_3$ coatings prepared under the arc current of 400A.

Figure 10 illustrates the decomposition characteristics of the acetaldehyde by TiO_2, TiO_2-30%$FeTiO_3$ and $FeTiO_3$ feedstock powders.

Although $FeTiO_3$ can absorb visible light, the initiated electron may easily recombine with a hole generated in

$FeTiO_3$. Thus the pure $FeTiO_3$ powder did not show photocatalytic activity. The photocatalytic activity of TiO_2 powder was higher than that of TiO_2-30%$FeTiO_3$ powder. Because the TiO_2-30%$FeTiO_3$ powder was manufactured by agglomeration of TiO_2 particles with $FeTiO_3$ particles using polyvinyl alcohol (PVA) as binder, the TiO_2 was separated from the $FeTiO_3$ particle by binder. Therefore, it is inferred that the initiated electron in the conduction band of TiO_2 can not transfer to the conduction band of $FeTiO_3$, which results in the relatively low photocatalytic activity of TiO_2-30%$FeTiO_3$ feedstock powder compared with that of the agglomerated TiO_2 powder. However, the PVA (C, H, O organic substance) has little influence on the properties of the sprayed coating, because PVA vaporizes over 550K and decomposes in the plasma spraying processes.

As a result, the compositions of the sprayed coatings have a great influence on the photocatalytic activity. Although pure $FeTiO_3$ compound has no photocatalytic property, the existence of $FeTiO_3$ could improve the photocatalytic activity of anatase TiO_2 if $FeTiO_3$ contacts coherently with TiO_2.

4. Conclusions

The composition and photocatalytic activity of plasma sprayed $FeTiO_3$, TiO_2-30%$FeTiO_3$ and TiO_2-50%$FeTiO_3$ coatings were investigated. The influence of $FeTiO_3$ compound on the photocatalytic activity of TiO_2 coating was clarified. The TiO_2-30%$FeTiO_3$ coating sprayed under an arc current of 400A had good photocatalytic activity because the coating did not contain the unfavorable Fe_2TiO_5 phase. However, the relative deposition speed of TiO_2-30%$FeTiO_3$ powder under the arc current of 400A, which was approximate to 4 μm/pass, was very low. Although pure $FeTiO_3$ compound nearly did not show photocatalytic performance, the existence of $FeTiO_3$ could improve the photocatalytic activity of anatase TiO_2 if the $FeTiO_3$ contacts coherently with TiO_2, and this was explained using a two-steps electron transfer model.

References

1) W. Q. Guo, S. Malus, D. H. Ryan, and Z. Altounian, Crystal structure and cation distributions in the $FeTiO_3$-Fe_2TiO_5 solid solution series, Journal of Physics Condensed Materials, Vol. 11 (1999) 6337-6347.
2) R. W. Taylor, Phase equilibria in the system FeO-Fe_2O_3-TiO_2 at 1573K, The American Mineralogist, Vol. 49 (1964) 1016-1030.
3) Y. Ishikawa and S. Akimoto, Magnetic properties of the $FeTiO_3$-Fe_2O_3 solid solution series, Journal of the Physical Society of Japan, Vol. 12(10) (1957) 1083-1098.
4) F. Zhou, S. Kotru, and R. K. Pandey, Pulsed laser-deposited ilmenite-hematite films for application in high-temperature electronics, Thin Solid Films, Vol. 408 (2002) 33-36.
5) P. F. McMonald, A. Parasiris, R. K. Pandey, B. L. Gries, and W. P. Kirk, Paramagnetic resonance and susceptibility of ilmenite, $FeTiO_3$ crystal, Journal of Applied Physics, Vol. 69 (2) (1991) 1104-1106.
6) Y. Ishikawa and S. Sawada, The study on substances having the ilmenite structure, physical properties of synthesized $FeTiO_3$ and $NiTiO_3$ ceramics, Journal of Physical Society of Japan, Vol. 11(5) (1956) 496-835.
7) Y. Ishikawa and S. Akimoto, Magnetic property and crystal chemistry of ilmenite ($FeTiO_3$) and hematite (Fe_2O_3) system, crystal chemistry, Journal of the Physical Society of Japan, Vol. 13(10) (1958) 1110-1118.
8) D. S. Ginley and M. A. Butler, The photoelectrolysis of water using iron titanate anodes, Journal of Applied Physics, Vol. 48(5) (1977) 2019-2021.
9) Y. Chen, Low-temperature oxidation of ilmenite ($FeTiO_3$) induced by high energy ball milling at room temperature, Journal of Alloys and Compound, Vol. 257 (1997) 156-160.
10) Y. Chen, Different oxidation reactions of ilmenite induced by high energy ball milling, Journal of Alloys and Compound, Vol. 266 (1998) 150-154.
11) F. -X. Ye and A. Ohmori, The photocatalytic activity and photo-absorption of plasma sprayed TiO_2-Fe_3O_4 binary oxide coatings, Surface and Coatings Technology, Vol.160 (2002) 62-67.
12) D. S. Ginley and M. A. Butler, The photoelectrolysis of water using iron titanate anodes, Journal of Applied Physics, Vol. 48(5) (1977) 2019-1021.